J Mater Sci: Mater Med (2011) 22:2735–2744
DOI 10.1007/s10856-011-4450-0

PLGA/Ag nanocomposites: in vitro degradation study and silver ion release

E. Fortunati · L. Latterini · S. Rinaldi · J. M. Kenny · I. Armentano

Received: 5 August 2011 / Accepted: 27 September 2011 / Published online: 15 October 2011

Abstract New nanocomposite films based on a biodegradable poly (DL-Lactide-co-Glycolide) copolymer (PLGA) and different concentration of silver nanoparticles (Ag) were developed by solvent casting. In vitro degradation studies of PLGA/Ag nanocomposites were conducted under physiological conditions, over a 5 week period, and compared to the behaviour of the neat polymer. Furthermore the silver ions (Ag^+) release upon degradation was monitored to obtain information on the properties of the nanocomposites during the incubation. The obtained results suggest that the PLGA film morphology can be modified introducing a small percentage of silver nanoparticles that do not affect the degradation mechanism of PLGA polymer in the nanocomposite. However results clearly evinced the stabilizing effect of the Ag nanoparticles in the PLGA polymer and the mineralization process induced by the combined effect of silver and nanocomposite surface topography. The Ag^+ release can be controlled by the polymer degradation processes, evidencing a prolonged antibacterial effect.

E. Fortunati · J. M. Kenny · I. Armentano (✉)
Materials Engineering Centre, UdR INSTM, NIPLAB, University of Perugia, Terni, Italy
e-mail: Ilaria.Armentano@unipg.it

L. Latterini · S. Rinaldi
Department of Chemistry and CEMIN, University of Perugia, Perugia, Italy

Present Address:
S. Rinaldi
Department of Chemistry, University of Siena, Via A. De Gasperi, 2 (Quartiere di S. Miniato), Siena 53100, Italy

Present Address:
J. M. Kenny
Institute of Polymer Science and Technology, ICTP-CSIC, Juan de la Cierva 3, Madrid, Spain

1 Introduction

Poly(DL-Lactide-co-Glycolide) (PLGA) copolymers have been widely utilized as biomaterials [1, 2] for implanted medical devices, e.g., endotrached tubes, urinary catheters, etc. [2–4]; however, such devices often cause bacterial infections limiting their applications [5]. Moreover, due to the non-bioactivity, they cannot bond directly with the bone and promote some mechanism as new bone formation on their surface at the early stage after implantation. Coating bone-like apatite on their surface through biomimetic process is considered a useful method to improve the bioactivity of polymer implants since bone-like apatite, particularly calcium-deficient and carbonated apatite, has been proven to be highly beneficial for bonding to bone compared with the current bioactive ceramics [6, 7].

Over the past decade nanocomposites obtained by dispersion of inorganic nanoparticles in polymeric matrices have attracted great interest, both in industry and in academia, because the presence of nanofillers affords a remarkable improvement of the material properties when compared to those of the virgin polymer or of conventional macro- and micro-composites. The improvements can include mechanical properties, heat resistance, flammability, gas permeability, and biodegradability of biodegradable polymers [8–11]. Moreover, the composites may show additional specific properties if the fillers are properly designed, e.g. linear and non-linear optical properties [12, 13] or biological activity. Metal nanoparticle filled polymers have attracted great interest for their unique optical, electrical, catalytic and biomedical properties [14, 15]. In particular, biodegradable nanocomposites based on metal nanoparticles as gold, titanium and silver, have

been applied as sensors or transducers, for the diagnosis and treatment of diseases [16, 17]. However the nanoparticles act as a filler of the polymer matrix thus affecting its morphology and structure which can result in a modification of the polymer properties [18, 19]. It has been recently demonstrated that loading PLGA with silver nanoparticles strongly reduced the bacterial development, mainly through a modification of the surface properties [20]. In particular, low concentrations of silver nanoparticles are able to induce surface morphological changes in the polymer film and affect surface nanocomposite wettability and roughness; all of these aspects influence the bacterial adhesion process on the nanocomposite surface [21]. These changes turn out in preventing bacterial colony growth and hence in an antibacterial action.

PLGA is a degradable polymer since in water media it undergoes hydrolytical chain scission and the mechanism of the degradation occurs in different steps involving water penetration, chain scission and transport phenomena of the products [22]. Several factors can affect the degradation rate of PLGA including chemical architecture [23–25] (e.g. molecular weight, length of lactic and glycolic blocks, ratio of lactic and glycolic acids), structure and morphology [26, 27] (e.g. crystallinity, shape of the specimen) and, therefore, the process technique [28–30] and the environment in which the polymer is placed [31, 32] (e.g.: body fluid, digestive fluid). When the water molecules attack the ester bonds in the polymer chains, the average length of the degraded chains becomes smaller. The process results in short oligomeric fragments having carboxylic end groups that render the polymer soluble in water. Very often, the molecular weight of some fragments are still relatively large such that the corresponding diffusion rates are slow. As a result, the remaining oligomers will lower the local pH, catalyze the hydrolysis of other ester bonds and speed up the degradation process. This mechanism is termed autocatalysis, which is frequently observed in thick biodegradable materials [33]. However, it has been reported that inorganic nanoparticles alter the degradation behaviour of PLGA since they can buffer the environment and reduce the autocatalytic action of the acid end groups created by chain scission [19]. Moreover, the dispersion of a reinforcement phase as Ag nanoparticles in the polymer and consequently the modification of surface properties, can induce changes in the polymer degradation process.

In this research, the degradation of PLGA/Ag nanocomposite films was investigated and compared to the behaviour of the neat polymer; furthermore the Ag^+ release upon degradation was monitored to obtain information on the degradation mechanism and on the properties of the nanocomposites during degradation.

2 Materials and methods

2.1 Materials

Poly(DL-Lactide-co-Glycolide) (PLGA) (I.V. 0.95−1.20 dl/g) ether terminated, an amorphous copolymer with a 50/50 ratio (PLA/PGA), was purchased from Absorbable Polymers-Lactel (Durect Corporation, UK). Commercial silver nanopowder (Ag), P203, with a size distribution ranged from 20 to 80 nm, was supplied by Cima NanoTech (Corporate Headquarters Saint Paul, MN USA).

2.2 Preparation of solvent cast PLGA/Ag films

Neat PLGA films were obtained by solvent casting, dissolving polymer granules in chloroform ($CHCl_3$) (10%w/v) and using a magnetic stirring at room temperature (RT) to obtain a complete polymer dissolution. PLGA nanocomposites were produced by dispersing the Ag powder in $CHCl_3$ at different percentages (0.1, 0.5 and 0.7% w/v), by means of sonication for 5 h (Ultrasonic bath-mod.AC-5, EMMEGI, Italy). The ultrasonic bath was used to improve the dispersion in the solvent promoting the following interaction with the biodegradable matrix. PLGA was mixed with Ag nanoparticles, by means of magnetic stirring until it was completely dissolved. Nanocomposite films were produced adding silver nanoparticles at 1, 5 and 7wt% (designed as PLGA/1Ag, PLGA/5Ag and PLGA/7Ag respectively) with respect to the polymer matrix. The dispersion was cast in a *Teflon*® sheet, to obtain films of rectangular shape (0.3 mm in thickness). Samples were air dried for 24 h, and for further 48 h in vacuum at 37°C, allowing the solvent to evaporate.

2.3 In vitro degradation studies

The degradation of the PLGA and PLGA/Ag films was investigated in phosphate buffered saline, PBS (1 l deionized H_2O, 80 g NaCl, 2 g KCl, 2.4 g KH_2PO_4, 11.45 g Na_2HPO_4) under physiological conditions (pH 7.4 and 37°C). Neat PLGA and nanocomposite samples (PLGA/1Ag, PLGA/5Ag and PLGA/7Ag) were maintained in PBS at 37°C for 5 weeks and the buffer solution was changed once a week. Sample weight loss, thermal, morphological and chemical changes were regularly analyzed over a 5 week period [34].

2.3.1 Thermal analysis (TGA)

Thermogravimetric analysis (TGA) was performed using a quartz rod microbalance (Seiko Exstar 6000, Cheshire, UK) on PLGA/Ag composite systems in the following conditions: 10 mg weight samples, nitrogen flow (250 ml/min), temperature range from 30 to 900°C, 10°C/min heating rate. Thermal degradation temperature (T_d) was evaluated from TGA thermograms.

2.3.2 Weight loss

Samples of neat polymer and nanocomposites with dimensions of 1 mm × 2 mm, 0.3 mm thick and weighing approxi 60 mg (M_0) were cut for the degradation experiments. At each time point, 5 samples of each formulation were removed from the buffer and weighed (M) after drying in vacuum for 1 h. The mass was measured to an accuracy of 0.01 mg using a Sartorius precision balance. Samples of each composition were measured and the results averaged. All measurements were expressed as an average ± the mean standard deviation.

2.3.3 FT-IR

Fourier infrared (FT-IR) spectra of the PLGA and nanocomposite films in the 400–4000 cm^{-1} range, were recorded using a Jasco FT-IR 615 spectrometer with attenuated total reflection spectroscopy (ATR).

2.3.4 Field emission scanning electron microscopy

Field emission scanning electron microscopy (FESEM, Supra 25-Zeiss, Germany) was used to examine the surface morphology of nanocomposite films before and after in vitro degradation. Energy dispersive X-ray spectroscopy (EDX INCA, Oxford Instruments, UK) was used to measure the chemical composition of samples after immersion in PBS. Surface of the samples were sputtered with gold and analyzed.

2.3.5 Optical absorption

The optical properties of silver nanoparticle suspensions were investigated by a Perkin–Elmer spectrophotometer (Lambda 800, USA). The absorption spectra of the solid samples before and after degradation, were recorded by a Varian (Cary 4000, USA) spectrophotometer which is equipped with a 150 mm integration sphere for reflectance spectra recording. A bar of barium sulphate was used as reference to calibrate the spectrophotometer. The recorded spectra were analyzed with the Kubelka–Munk equation in order to make possible the comparison among different samples.

2.4 Silver ion release

The release of metal cation (Ag^+) by the composite materials was monitored by Varian 700-ES series Inductively Coupled Plasma-Optical Emission Spectrometers (ICP-OES) analyzing solutions obtained by the interaction of the solvent with the nanocomposite samples at different times. In order to avoid any interferences between ICP measurements and the present in buffers, the polymer degradation effects on the Ag^+ release was carried out in water solutions. In particular, nanocomposites samples (area 2 cm^2) were incubated in 15 ml of deionized water for up to 100 days to monitor the amount of silver ions released upon polymer degradation; the solutions were stored at 37° C in dark conditions. The solutions were regularly analyzed by ICP to determine the concentration of Ag^+, once the instrumental setup has been calibrated with a standard solution. Experiments were conducted in duplicate. The obtained Ag^+ concentrations recorded were then correlated with the degradation time.

3 Results and discussion

3.1 In vitro degradation study

In vitro degradation studies were conducted by weight loss measurements, thermal degradation, infrared spectroscopy, physical alterations and FESEM imaging performed as a function of the incubation time.

3.1.1 Thermogravimetric investigations

The effects of the hydrolytic degradation on the thermal behaviour of PLGA and PLGA/Ag nanocomposites were investigated at different incubation times and the TGA results are reported in Fig. 1. The obtained derivative curves (DTG) for PLGA and PLGA/7Ag nanocomposites before and at different incubation times were reported in Fig. 1a. Pristine PLGA degrades with a single peak at about 365°C with a shoulder at lower temperature ranged from 250 to 320°C, in agreement with literature data [20, 34]. Before hydrolysis process, silver nanoparticles have a very little influence on the thermal degradation of PLGA, with an evident slight decrease (10°C) in degradation temperature (T_d) only in nanocomposite with the higher silver nanoparticle content (7 wt%) [20, 34] indicating that the thermal degradation of PLGA/Ag systems occurs according to the typical PLGA chain scission mechanism (Fig. 1a). The small difference in the degradation

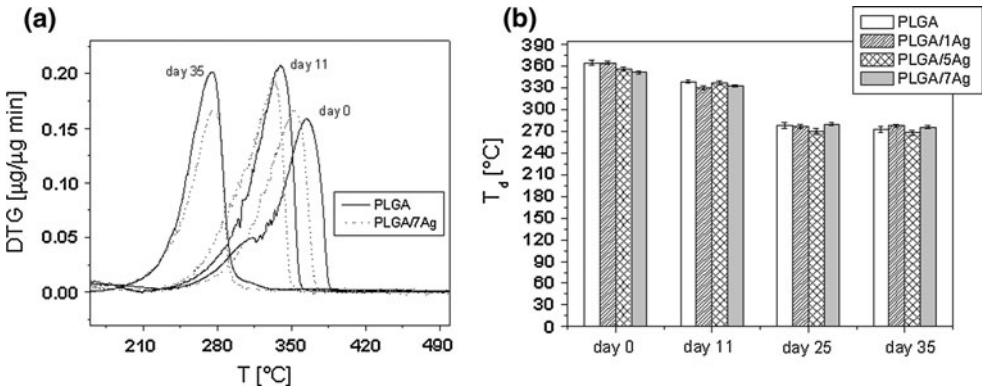

Fig. 1 Derivative oxidation thermograms of degraded PLGA and, PLGA/7Ag nanocomposites (**a**). Thermal degradation temperature vs incubation time (**b**)

temperatures between neat PLGA and PLGA/Ag nanocomposites, observed before and after 11 days of incubation, decreases with the incubation time (at 25 or 35 days of incubation), highlighting a stabilizing effect of the silver nanoparticles during the degradation pattern. Moreover, the DTG curves for PLGA/Ag nanocomposites exhibit broader thermal decomposition ranges than pure PLGA, before and during the degradation process. This can be caused by a thermal effect occurring in the polymer, influenced by particle distributions within the PLGA during sample preparation, as already reported for similar system by Yeo et al. [35]. After 35 days of incubation a sharp peak was revealed in all the systems, when the polymer chain scission became the main effect.

Figure 1b shows the degradation temperature values for PLGA and for all PLGA/Ag formulations at different incubation times. The T_d decreases of about 10°C after 11 days of incubation, in all the systems. The degradation process become evident between 25 and 30 days in vitro with a shift of 90°C in degradation temperature. The shift to lower temperatures of the PLGA thermal degradation peak is clearly associated to the reduction of the molecular weight of the matrix as a consequence of the hydrolytic behaviour after exposure to PBS [34].

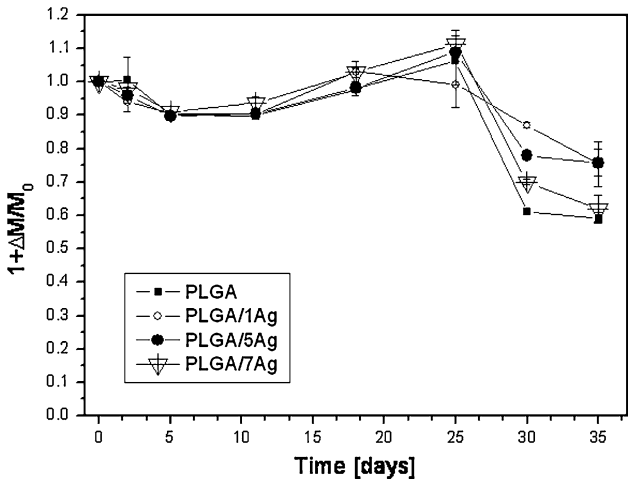

Fig. 2 Weight loss of degrading PLGA and PLGA/Ag nanocomposite films as a function of incubation time in PBS

3.1.2 Weight loss

Figure 2 displays the weight loss of the degrading PLGA and PLGA/Ag nanocomposite films with different silver nanoparticle content as a function of the incubation time in PBS at 37°C. The dynamics of weight loss for all the nanocomposites are similar to the neat PLGA behaviour during hydrolytic degradation process. Initially, for all the material studied, there is a gradual and slight reduction of the sample weight that continues for several days. Considering the experimental error reported for mass loss values, from 10 to 25 days of in vitro degradation, all the samples maintained a constant weight but, after 1 month of incubation, a dramatic decrease in mass is observed in agreement with previous studies on other PLGA based composites [34, 36, 37]. Moreover, the presence of silver nanoparticles does not significantly affect the weight loss of the polymer matrix at 37°C, and a similar trend of weight loss against time of degradation can be observed for all the studied materials, within the experimental errors.

3.1.3 Infrared spectroscopy

FT-IR spectra of PLGA copolymer and PLGA/Ag nanocomposites at different silver content and at different incubation times were recorded. As previously reported, IR spectra were monitored in four different regions: the first one refers to the aliphatic C–H stretching vibrations between 3000 and 2850 cm^{-1}, the second and third regions include the C=O stretching bands at 1850–1650 cm^{-1} and the asymmetric C–O stretching vibrations at 1300–1000 cm^{-1}, respectively; the fourth is the OH stretching region at 3700–3400 cm^{-1} [38, 39].

Figure 3 shows FT-IR/ATR spectra of PLGA (Fig. 3a) and PLGA/7Ag (Fig. 3b) samples after different incubation times. Figure 3a demonstrates that no significant changes are present in the behaviour of PLGA at 5 days of

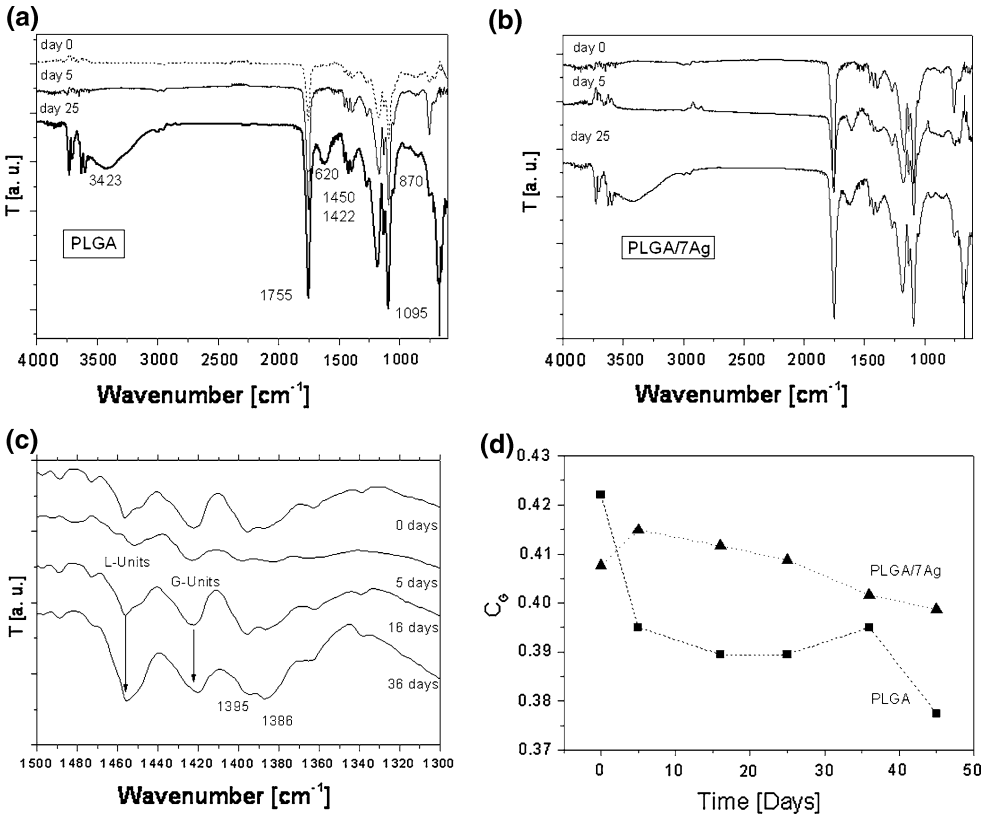

Fig. 3 FT-IR/ATR spectra of PLGA (**a**), and PLGA/7Ag (**b**), samples for different incubation times. Infrared spectra (1500–1300 cm^{-1} region) collected for PLGA nanocomposite films degraded in 20 ml PBS at different degradation times (**c**). Relative glycolic unit content, CG, of remaining polymer versus degradation time for PLGA films degraded in 20 ml PBS at 37°C (**d**)

incubation respect to pristine PLGA and a similar trend was detected for PLGA/7Ag (Fig. 3b) and the other nanocomposites (data not shown) until 3 weeks of in vitro degradation. Starting from 25 days of incubation, some differences in the peak intensity appear in the region of the characteristic carbonyl stretching vibrations between 1850 and 1650 cm^{-1}. The spectra showed an absorption increase in the frequency regions where the carbonyl (C=O) and the OH stretching absorb, the latter appearing as broad band centred at 3400 cm^{-1} [40, 41]. The signals are due to the hydrolitic process leading to the formation of carboxylic acid end chains which is occurring in the neat PLGA and in the composites in a similar time-scale. To evaluate in deeper details the degradation process the IR spectra were monitored in the 1500–1300 cm^{-1} region for nanocomposite samples at different degradation times (Fig. 3c). In this region, two bands are observed at 1452 cm^{-1} and 1422 cm^{-1} which correspond to the asymmetric bending of CH_3 from the lactic units and the bending of CH_2 from the glycolic units of the polymer, respectively. The relative intensities of these two bands were used to estimate the relative quantity of glycolic (C_G) and lactic (C_L) units present in the sample. For this purpose the two bands were de-convoluted and their intensity estimated. The relative quantity of lactic, C_L, and glycolic, C_G, units present in our samples was obtained through

$$C_G = \frac{I_{1422}}{I_{1422} + I_{1452}}, \quad C_L = \frac{I_{1452}}{I_{1422} + I_{1452}} \tag{1}$$

where I_{1422} is the intensity of the band at 1422 cm^{-1} and I_{1452} is the intensity of the band at 1452 cm^{-1}. The variation of C_G as a function of the degradation time for PLGA and PLGA/7Ag nanocomposites is given in Fig. 3d. As can be seen the relative quantity of glycolic units decrease in the PLGA neat polymer already during the first week of degradation, as expected confirming the preferential degradation of these units. The remaining polymer, therefore, becomes richer in lactic units [42]. In PLGA/7Ag nanocomposite a less evident decrease was measured, evidencing the stability effect of the silver nanoparticles during polymer degradation and confirming the TGA results.

3.1.4 Physical and morphological alterations

The gross appearance of all PLGA systems changed during degradation. The amorphous PLGA samples were initially almost transparent. As degradation proceeded, they became whitish due to water absorption. Then became brittle and began to disintegrate in agreement with previous publications [43]. The visual aspects of PLGA and PLGA/Ag nanocomposite films during degradation seem to be

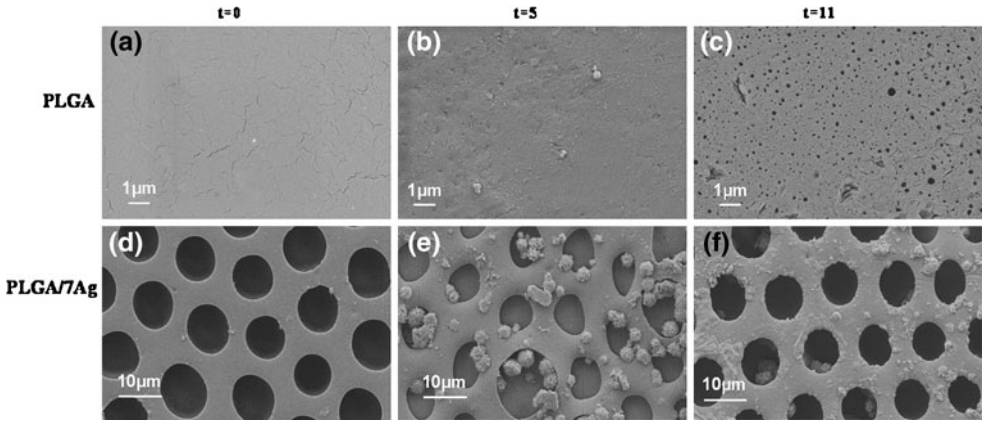

Fig. 4 FESEM images of pristine PLGA and PLGA/7Ag films (**a, d**), after 5 days (**b, e**), and after 11 days (**c, f**) of degradation

similar. The higher opacity for samples upon degradation has been reported due to various phenomena, such as an enhancement of the light diffusion through the material for the presence of water and/or degradation products formed [44–46], and to the formation of micro holes and cracks in the bulk of the specimen during degradation of the polymer matrix.

The changes in surface morphology caused by the hydrolysis were observed using a Field Emission Scanning Electron Microscopy (FESEM). Figure 4 shows the FESEM images of PLGA neat film and PLGA/7Ag nanocomposite before and after different incubation times in PBS at 37°C. FESEM observations were conducted until 11 days of incubation since after this period the samples lost their stiffness and the FESEM observation became difficult.

FESEM images show the formation of superficial defects due to degradation just after 5 days of incubation in vitro for PLGA neat films since the appearance of micro-holes and cracks on the film surface were observed. At longer incubation times the defects appeared much more enlarged confirming the continuation of the degradation process. The FESEM images recorded on the upper surface of PLGA/7Ag system (Fig. 4) show the odd topography previously described [20]. Upon exposure to the degrading environment a round off of the pore edges was observed and no other defects were detected, thus suggesting that the degradation process is essentially localized in pore proximity. Furthermore, particle-like structures are observable around the pore edges as a consequence of the incubation in PBS [47]. These micron-size particles are better observed in PLGA/7Ag images recoded at higher

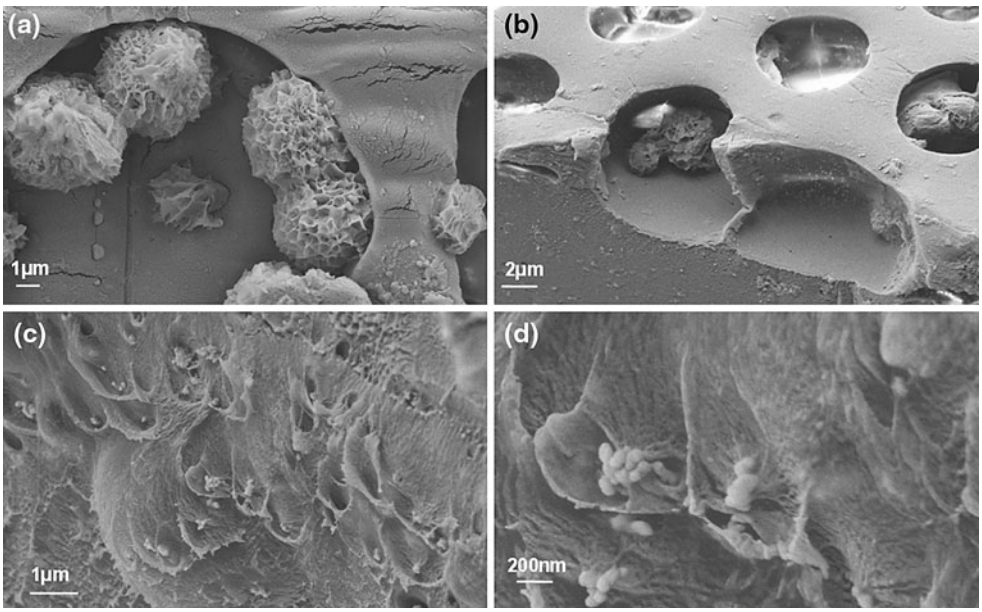

Fig. 5 FESEM images of PLGA/7Ag nanocomposite surface after 5 days (**a**), and after 11 days (**b, c, d**) of degradation

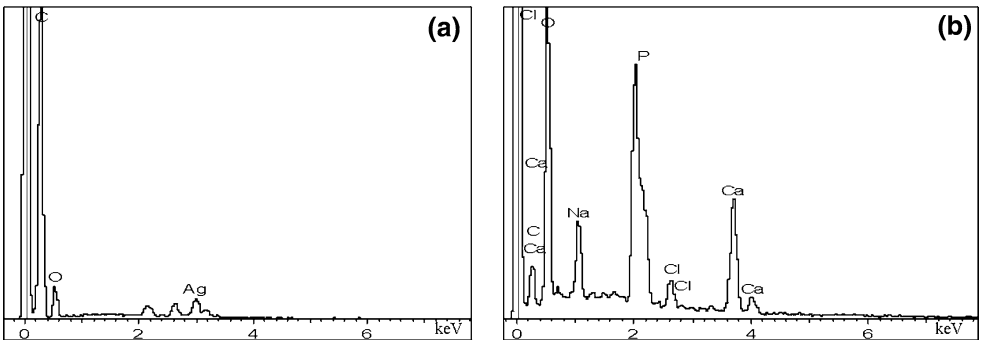

Fig. 6 EDX spectra of PLGA/7Ag nanocomposite surface as prepared (**a**), and after 11 days (**b**) of degradation

magnification (Fig. 5a, b) after 5 and 11 days in vitro, where the presence of these structures inside the superficial pores is evident. Moreover, observing the lateral surface of PLGA/Ag nanocomposite at 11 days in vitro, it is possible to see the presence of silver nanoparticles on the pore wall as a consequence of polymer chain degradation process (Fig. 5b−d).

Figure 6 shows EDX spectra of PLGA/7Ag surface pristine (a) and after 11 days of incubation (b). The analysis shows strong peaks due to calcium and phosphorus on the surface of nanocomposite after 11 days of incubation, with calcium-phosphorus atomic ratios of 1.36. The ratio is close to that of octacalcium phosphate (OCP, Ca8(HPO4)2(PO4)4_5H2O, Ca/*P* = 1.33). These findings suggest that the specific surface chemistry and topography with regular pore structure of PLGA/Ag composites assisted the nucleation of mineral nanocrystals and the mineralization process. This apatite-forming ability is presumably due to interactions of the buffer ions (see experimental section for composition) with the surface pores of nanocomposites, which are favoured by the degradation of the PLGA surface layer and are assisted by the presence of Ag nanoparticles (Fig. 5c−d). In contrast, apatite particles did not form on PLGA neat films [48].

3.1.5 *Optical absorption*

The absorption spectra of pristine PLGA and PLGA/Ag nanocomposites before and after exposure to hydrolytic medium are shown in Fig. 7. PLGA/Ag nanocomposites before degradation (Fig. 7a) present absorption bands at 300 and 375 nm which are assigned to plasmon bands (SPR) of the nanoparticles (Fig. 7a insert), since the polymer contribution is at lower wavelengths [20]. It has to be noted that the SPR absorption in the composites appeared red shifted compared to the spectra recorded on the neat Ag particles in suspensions; this behaviour can be due to changes in the refractive index of the medium around the metal particles, as reported in the literature [49–51]. Once the nanocomposites were exposed to the hydrolytic environment, a significant enhancement of the SPR bands (Fig. 7b), respect to the intensity before the exposure to the medium, was observed. This behaviour is likely due to an alteration of the particle environments induced by degradation of polymer matrix which resulted in a reduction of the screening effects imposed by the matrix, as already supported by FESEM images. Furthermore, the SPR bands of the metal nanoparticles are blue shifted (ca. 10 nm) in degraded nanocomposite

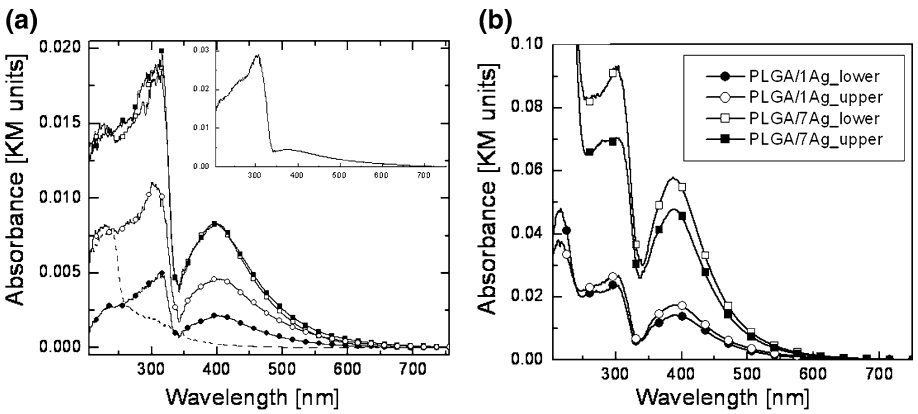

Fig. 7 UV–vis absorption spectra of materials (**a**), before incubation and (**b**), after 20 days of incubation. *Panel a*: PLGA (*dotted line*), PLGA/1Ag (*circles*) and PLGA/7Ag (*squares*) recorded at the lower (*full symbols*) and upper (*empty symbols*) surfaces; insert: absorption spectra of silver nanoparticles. *Panel b*: PLGA/1Ag (*circles*) and PLGA/7Ag (*squares*) recorded at the lower (*full symbols*) and upper (*empty symbols*) surfaces after 20 days of exposure to the degradation environment

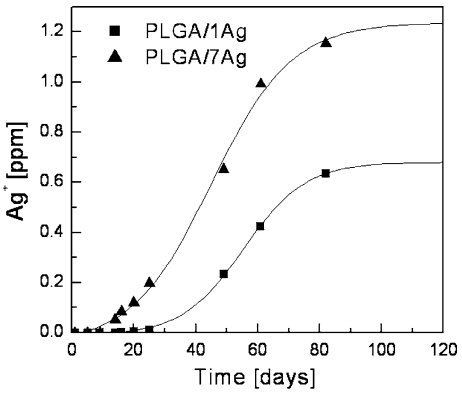

Fig. 8 Ag^+ release upon degradation of PLGA/1Ag and PLGA/7Ag nanocomposites

compared to the spectra of the original nanocomposites; this observation together with the spectrum of the neat nanoparticles in water, indicated a closer contact of the metal with the aqueous medium. Optical absorption results are in agreement with the morphological outcomes, confirming the superficial presence of silver nanoparticles as a consequence of polymer chain degradation process.

3.2 Silver ion release

Silver ion (Ag^+) release from the PLGA/Ag nanocomposites with 1 and 7wt% of nanoparticles was investigated once the nanocomposites with different particle loadings were exposed to the hydrolytic environment. The silver ion content in aqueous solutions was regularly monitored in time to check the relation between the ion release and the polymer degradation process. Figure 8 shows the concentration of Ag^+ detected in the solutions where the PLGA/Ag nanocomposites with 1 or 7wt% of nanoparticles, respectively, were incubated as a function of time. For both nanocomposite samples the amount of detected Ag^+ is characterized by a sigmoid trend [52], although the absolute quantity is dependent on the silver loading. Moreover, the release was relatively slow at early stage of incubation and it became faster after 20 days of exposure to the hydrolytic environment, when an evident weight loss of the samples, due to the PLGA random chain scission, was clearly measurable.

The lower release rate at the beginning of degradation can be explained on the basis of the shielding action of the polymer film which reduces the nanoparticle-water contact thus the particle oxidation is initially controlled by the polymer permeation to water hence making slow the cation release. ICP measurements indicated that the amount of Ag^+ detected increased with the incubation time, thus the rate of Ag^+ release is enhanced by the polymer degradation. A similar behaviour is observed for both the composites although the amount of detected Ag^+ is higher for PLGA/7Ag.

In particular, at the 13th day of incubation, the rate of Ag^+ release started to increase; afterwards the oxidation of Ag nanoparticles occurred in a massive manner following the polymer hydrolysis process. The release rate started to decrease after 70 days of incubation becoming negligible after 80 days of exposure. The Ag^+ release by the composites in solution is correlated with the polymer degradation process and the release could be controlled by engineering of system composition and surface properties. Moreover, the release of cationic silver can electrostatically assist the deposition and growth of calcium phosphate crystals, although at this stage the effects of the surface porosity cannot be decoupled.

4 Conclusions

The reported results imply that PLGA properties can be modified introducing a small percentage of silver nanoparticles and that the Ag nanoparticles do not affect the overall degradation mechanism of PLGA. Furthermore, a stabilizing effect of Ag nanoparticles is clearly evinced. The presence of Ag nanoparticles also induces a mineralization process when nanocomposite samples are immersed in the PBS buffer as a consequence of the combined effect of silver nanoparticles and the induced nanocomposite surface topography. The Ag^+ release in solution can be controlled by the polymer degradation processes, evidencing a possible prolonged antibacterial effect, during PLGA immersion.

The results of this research suggest that the combination of biodegradable polymers and silver nanoparticles opens a new perspective for the use of nanomaterials with tunable properties obtaining antimicrobial surfaces for biomedical applications.

Acknowledgments The authors gratefully acknowledge the financial support from INSTM.

References

1. Ma PX. Scaffold for Tissue Engineering. Materials Today. 2004;7:30–40.
2. Park GE, Pattison MA, Park K, Webster TJ. Accelerated chondrocyte functions on NaOH-treated PLGA scaffolds. Biomaterials. 2005;26:3075–86.
3. Sun B, Ranganathan B, Feng SS. Multifunctional poly(DL-Lactide-co-glycolide)/montmorillonite (PLGA/MMT) nanoparticles decorated by Trastuzumab for targeted chemotheraphy of breast cancer. Biomaterials. 2008;29:475–86.
4. Wang Y, Challa P, Epstein DL, Yuan F. Controlled release of ethacrynic acid from poly(lactide- *co*-glycolide) films for glaucoma treatment. Biomaterials. 2004;25:4279–85.

5. Darouiche RO. Anti-Infective Efficacy of Silver-Coated Medical Prostheses. Clin Infect Dis. 1999;29:1371–7.
6. Ohura K, Nakamura T, Yamamuro T. Bone-bonding ability of P2O5-free CaO.SiO2 glasses. J Biomed Mater Res. 1991;25:357–65.
7. Neo M, Kotani S, Nakamura T. A comparative study of ultrastructure of the interfaces between four kinds of surface-active ceramic and bone. J Biomed Mater Res. 1992;26:1419–32.
8. Bockstaller MR, Mickiewicz RA, Thomas EL. Block copolymer nanocomposites: perspectives for tailored functional materials. Adv. Mater. 2005;17:1331–49.
9. Tjong SC. Structural and mechanical properties of polymer nanocomposites. Mater. Sci. Eng. R. 2006;53:73–197.
10. Mai YW, Yu ZZ, editors. Polymer nanocomposites. Chambridge: RCR Press; 2006.
11. Aloisi GG, Costantino U, Latterini L, Nocchetti M, Camino G, Frache A. Preparation and spectroscopic characterisation of intercalation products of clay and of clay-polypropylene composites with rhodamine B. J. Phys. Chem. Solids. 2006;67: 909–14.
12. Aloisi GG, Elisei F, Nocchetti M, Camino G, Frache A, Costantino U, Latterini L. Mater. Chem. Phys. 2010;123:3777–9.
13. Latterini L, Nocchetti M, Costantino U, Aloisi GG, Elisei F. Organized chromophores in layered inorganic matrices. Inorg Chim Acta. 2007;360:728–40.
14. Lee JY, Nagahata JLR, Horiuchi S. Effect of metal nanoparticles on thermal stabilization of polymer/metal nanocomposites prepared by a one-step dry process. Polymer. 2006;47:7970–9.
15. Gautam A, Ram S. Preparation and thermomechanical properties of Ag-PVA nanocomposite films. Mater. Chem. Phys. 2010;119: 266–71.
16. Wang JF, Liu XY, Loan B. Fabrication of Ti/polymer biocomposites for load-bearing implant applications. J. Mater. Process. Tech. 2008;1–3:428–33.
17. Ren J, Hong H, Ren T, Teng T. Preparation and characterization of magnetic PLA-PEG composite nanoparticles for drug targeting. React Funct Polym. 2006;66:944–51.
18. Palza H, Vergara R, Zapata P. Macromol Mater Eng. 2010;295:899–905.
19. Yang Z, Best SM, Cameron RE. Adv. Mater. 2009;21:1900–4.
20. Armentano I, Fortunati E, Latterini L, Rinaldi S, Saino E, Visai L, Elisei F, Kenny JM. J. Nanostruc. Polym. Nanocomp. 2010; 6(4):110–8.
21. An YH, Friedman RJ. Concise review of mechanism of bacterial adhesion of biomaterials surface. J Biomed Mater Res. 1998;43:338–48.
22. Kulkarni A, Reiche J, Lendlein A. Hydrolytic degradation of poly(*rac*-lactide) and poly[(*rac*-lactide)-co-glycolide] at the air-water interface. InterfaceAnal. 2007;39:740–6.
23. Cam D, Hyon SH, Ikada Y. Degradation of high-molecular-weight poly(L-Lac-tide) in alkaline medium. Biomaterials. 1995;16(11):833–43.
24. Heya T, Okada H, Ogawa Y, Toguchi H. Factors influencing the profiles of TRH release from co-poly(DL-lactic-glycolic acid) microspheres. Int J Pharm. 1991;72(3):199–205.
25. Omelczuk MO, McGinity JW. The influence of polymer glass-transition temperature and molecular-weight on drug release from tablets containing poly(DL-lactic acid). Pharm Res. 1992;9(1):26–32.
26. Fu BX, Hsiao BS, Chen G, Zhou J, Koyfman I, Jamiolkowski DD, et al. Structure and property studies of bioabsorbable poly(glycolide-co-lactide) fiber during processing and in vitro degradation. Polymer. 2002;43(20):5527–34.
27. Hurrell S, Cameron RE. The effect of initial polymer morphology on the degradation and drug release from polyglycolide. Biomaterials. 2002;23(11):2401–9.
28. Lu L, Garcia CA, Mikos AG. In vitro degradation of thin poly(DL-lactic-co-glycolic acid) films. J Biomed Mater Res. 1999;46(2):236–44.
29. Panyam J, Dali MA, Sahoo SK, Ma WX, Chakravarthi SS, Amidon GL, et al. Polymer degradation and in vitro release of a model protein from poly(DL-Lactide-co- glycolide) nano- and microparticles. J Control Release. 2003;92(1–2):173–87.
30. Williams HE, Huxley J, Claybourn M, Booth J, Hobbs M, Meehan E, et al. The effect of gamma-irradiation and polymer composition on the stability of PLGA polymer and microspheres. Polym Degrad Stab. 2006;91(9):2171–81.
31. Chu CC. An in vitro study of the effect of buffer on the degradation of poly(-glycolic acid) sutures. J Biomed Mater Res. 1981;15(1):19–27.
32. Chu CC. The in vitro degradation of poly(glycolic acid) sutures-effect of pH. J Biomed Mater Res. 1981;15(6):795–804.
33. Bikiaris DN, Chrissafis K, Paraskevopoulos KM, Triantafyllidis KS, Antonakou EV. Investigation of thermal degradation mechanism of an aliphatic polyester using pyrolysis–gas chromatography–mass spectrometry and a kinetic study of the effect of the amount of polymerisation catalyst. Polym Degrad Stab. 2007;92:525–36.
34. Armentano I, Dottori M, Puglia D, Kenny JM. Effects of carbon nanotubes (CNTs) on the processing and in vitro degradation of poly(DL-lactide-*co*-glycolide)/CNT films. J Mater Sci Mater Med. 2008;19:2377–87.
35. Yeo SY, Tan WL, Bakar M Abu, Ismail J. Silver sulfide/poly(3-hydroxybutyrate) nanocomposites: Thermal stability and kinetic analysis of thermal degradation. Polym Degrad Stab. 2010;95: 1299–304.
36. Lusa LU, Garcia CA, Mikos AG. In vitro degradation of thin poly(DL-lactic-co-glycolic acid) films. J Biomed Mater Res. 1999;46:236–44.
37. Siepmann J, Elkharraz K, Siepmann F, Klose D. How autocatalysis accelerates drug release from PLGA-based microparticles: a quantitative treatment. Biomacromolecules. 2005;6:2312–9.
38. Aguilar CA, Lu Y, Mao S, Chen S. Direct micro-patterning of biodegradable polymers using ultraviolet and femtosecond lasers. Biomaterials. 2005;26:7642–9.
39. Kister G, Cassanas G, Vert M. Morphology of poly(glycolic acid) by IR and Raman spectroscopies. Spectrochim. Acta Part. A. 1997;53:1399–403.
40. Mercado AL, Allmond CE, Hoekstra JG, Fitz-Gerald JM. Pulsed laser deposition vs. matrix assisted pulsed laser evaporation for growth of biodegradable polymer thin films. Appl. Phys. A Mater. Sci. Process. 2005;81:591–9.
41. Huang MH, Li S, Vert M. Synthesis and degradation of PLA-PCL-PLA triblock copolymer prepared by successive polymerization of caprolactone and DL-Lactide. Polymer. 2004;45:8675–81.
42. Vey E, Roger C, Meehan L, Booth J, Claybourn M, Miller AF, Spiani A. Degradation mechanism of poly(lactic-co-glycolic) acid block copolymer cast films in phosphate buffer solution. Polym Degrad Stab. 2008;93:1869–76.
43. Loo SCJ, Ooi CP, Boey YCF. Radiation effects on poly(lactide-*co*-glycolide) (PLGA) and poly(L-lactide) (PLLA). Polym Degrad Stab. 2004;83:259–65.
44. Jarerat A, Tokiwa Y. Degradation of poly (L-lactide) by a fungus. Macromol Biosci. 2001;1:136–40.
45. Jarerat A, Pranamuda H, Tokiwa Y. Poly(L-lactide)-degrading activity in various actinomycetes. Macromol Biosci. 2002;2: 420–8.
46. Torres A, Li SM, Roussos S, Vert M. Poly (lactic acid) degradation in soil or under controlled conditions. J. of Applied Polymer Science. 1996;62:2295–302.
47. Qu X, Cui W, Yang F, Min C, Shen H, Bei J, Wang S. The effect of oxygen plasma pretreatment and incubation in modified

simulated body fluids on the formation of bone-like apatite on poly(lactide-*co*-glycolide) (70/30). Biomaterials. 2007;28:9–18.
48. Lee JC, Cho SB, Lee SJ, Rhee SH. Nucleation and growth mechanism of apatite on a bioactive and degradable ceramic/polymer composite with a thick polymer layer. J Mater Sci. 2009;44:4531–8.
49. Kulkarni AP, Munechika K, Noone KM, Smith JM, Ginger DS. Phase Transfer of Large Anisotropic Plasmon Resonant Silver Nanoparticles from Aqueous to Organic Solution. Langmuir. 2009;25:7932–9.
50. Kazim S, Pfleger J, Prochazka M, Bondarev D, Vohlidal J. New Phosphorus-Containing Spherical Carbon Adsorbents as Promising Materials in Drug Adsorption and Release. Coll. Interf. Sci. 2011;354:611–9.
51. Kubo S, Diaz A, Tang Y, Mayer TS, Khoo IC, Mallouk TE. Tunability of the Refractive Index of Gold Nanoparticle Dispersions. Nano Lett. 2007;7:3418–23.
52. Benn TM, Westerhoff P. Nanoparticle silver released into water from commercially available sock fabrics. Environ Sci Technol. 2008;42:7025–6.